

Overdosage of Balanced Protein Complexes Reduces Proliferation Rate in Aneuploid Cells

Highlights

- Cells with complex aneuploidies ($2n + x$) have many balanced $3n$ protein complexes
- In contrast to $3n$ subunits of imbalanced complexes, balanced complexes are not degraded
- The “Overdosage Hypothesis”: $3n$ balanced protein complexes inhibit proliferation
- $3n$ balanced protein complexes are selected against in human cancers

Authors

Ying Chen, Siyu Chen, Ke Li, ..., Yingchun Wang, Lucas B. Carey, Wenfeng Qian

Correspondence

lucas.carey@pku.edu.cn (L.B.C.), wfqian@genetics.ac.cn (W.Q.)

In Brief

Tumor cells often exhibit karyotypical abnormalities involving multiple chromosomes. However, it remains unclear why karyotype affects proliferation. Chen et al. generated 92 cancer-like yeast strains with complex aneuploidies ($2n + x$) and propose a new hypothesis as to why these cells exhibit proliferation defects: overdosage of $3n$ balanced protein complexes inhibits proliferation, likely through disrupting the stoichiometric balance among components of certain signaling pathways.



Overdosage of Balanced Protein Complexes Reduces Proliferation Rate in Aneuploid Cells

Ying Chen,^{1,3,4} Siyu Chen,^{1,3,4} Ke Li,^{1,3} Yuliang Zhang,^{1,3,4} Xiahe Huang,^{2,3} Ting Li,² Shaohuan Wu,^{1,3,4} Yingchun Wang,^{2,3} Lucas B. Carey,^{5,6,7,*} and Wenfeng Qian^{1,3,4,*}

¹State Key Laboratory of Plant Genomics, Institute of Genetics and Developmental Biology, Chinese Academy of Sciences, Beijing 100101, China

²State Key Laboratory of Molecular Developmental Biology, Institute of Genetics and Developmental Biology, Chinese Academy of Sciences, Beijing 100101, China

³Key Laboratory of Genetic Network Biology, Institute of Genetics and Developmental Biology, Chinese Academy of Sciences, Beijing 100101, China

⁴University of Chinese Academy of Sciences, Beijing 100049, China

⁵Department of Experimental and Health Sciences, Universitat Pompeu Fabra, Barcelona 08003, Spain

⁶Center for Quantitative Biology and Peking-Tsinghua Center for Life Sciences, Academy for Advanced Interdisciplinary Studies, Peking University, Beijing 100871, China

⁷Lead Contact

*Correspondence: lucas.carey@pku.edu.cn (L.B.C.), wfqian@genetics.ac.cn (W.Q.)

<https://doi.org/10.1016/j.cels.2019.06.007>

SUMMARY

Cells with complex aneuploidies display a wide range of phenotypic abnormalities. However, the molecular basis for this has been mainly studied in trisomic ($2n + 1$) and disomic ($n + 1$) cells. To determine how karyotype affects proliferation in cells with complex aneuploidies, we generated 92 $2n + x$ yeast strains in which each diploid cell has between 3 and 12 extra chromosomes. Genome-wide and, for individual protein complexes, proliferation defects are caused by the presence of protein complexes in which all subunits are balanced at the 3-copy level. Proteomics revealed that over 50% of 3-copy members of imbalanced complexes were expressed at only $2n$ protein levels, whereas members of complexes in which all subunits are stoichiometrically balanced at 3 copies per cell had $3n$ protein levels. We validated this finding using orthogonal datasets from yeast and from human cancers. Taken together, our study provides an explanation of how aneuploidy affects phenotype.

INTRODUCTION

Aneuploidy refers to karyotypes that are not an exact multiple of the haploid genome (Birchler and Veitia, 2007; Täckholm, 1922; Torres et al., 2008, 2010b) and is a hallmark of tumor cells (Albertson et al., 2003; Holland and Cleveland, 2009; Siegel and Amon, 2012; Weaver and Cleveland, 2006). At the cellular level, aneuploidy usually exhibits a reduced proliferation rate (Birchler and Veitia, 2012; Torres et al., 2008). For example, in the budding yeast *Saccharomyces cerevisiae*, the proliferation rate of aneuploidy is reduced significantly under non-stress con-

ditions (Parry and Cox, 1970; Pavelka et al., 2010). Similar observations were also reported in the fission yeast *Schizosaccharomyces pombe* (Niwa et al., 2006; Niwa and Yanagida, 1985) and mammalian cells (Baker et al., 2004; Segal and McCoy, 1974; Stingle et al., 2012; Thompson and Compton, 2008; Williams et al., 2008). Aneuploidy has also been suggested to suppress the proliferation of tumor cells (Sheltzer et al., 2017). The apparent fast expansion of tumor cell population is likely because mutations in cell-cycle-related genes remove the proliferative restrictions imposed on individual cells in multicellular organisms, obscuring the adverse effect of aneuploidy (Holland and Cleveland, 2009; Torres et al., 2008, 2010b).

Although the reduced proliferation rate has been observed in many types of aneuploid cells, the mechanistic link between the two remains under investigation. Two mutually non-exclusive hypotheses have been proposed. The balance hypothesis asserts that the disruption of the stoichiometric relationship among subunits in a macromolecular complex perturbs its function and can cause cytotoxicity (Birchler and Veitia, 2007, 2010; Papp et al., 2003; Veitia, 2002, 2005). Consistent with the balance hypothesis, gain or loss of some chromosomes in a genome usually results in greater growth defects than complete duplication of all chromosomes (Birchler and Veitia, 2010; Otto and Whitton, 2000). In addition, the overexpression of the α -tubulin gene can partly rescue the lethality caused by the overexpression of the β -tubulin gene (Abruzzi et al., 2002; Katz et al., 1990), demonstrating the importance of dosage balance within a protein complex. The burden hypothesis was proposed based on the observation that aneuploid cells were under proteotoxic stress (Oromendia et al., 2012), which implies that the folding and degradation of the extra protein subunits are a burden to aneuploid cells (Dephoure et al., 2014; Geiler-Samerotte et al., 2011; Torres et al., 2010b). In fact, 50% to 70% of extra subunits in an imbalanced complex are degraded (Dephoure et al., 2014; Ishikawa et al., 2017). For example, histone and ribosomal proteins that are not assembled are rapidly degraded (Abovich et al., 1985; Agrawal and Bowman, 1987; elBaradi et al., 1986;



Gunjan and Verreault, 2003; Maicas et al., 1988; Warner et al., 1985). Related to this, aneuploid cells are more sensitive to drugs inhibiting protein folding or proteasome function (Sheltzer et al., 2011; Torres et al., 2007; Whitesell and Lindquist, 2005). Both balance and burden hypotheses explain why stoichiometric imbalance leads to reduced fitness.

Previous studies investigating the causes of the reduction in proliferation rate in aneuploid cells were mainly conducted in disomic ($n + 1$) or trisomic ($2n + 1$) aneuploid cells (Dephousse et al., 2014; Oromendia and Amon, 2014; Oromendia et al., 2012; Stingelet et al., 2012; Thorburn et al., 2013; Torres et al., 2010a, 2007; Williams et al., 2008). In $n + 1$ or $2n + 1$ cells, both the balance hypothesis and the burden hypothesis predict that proliferation rate will decrease as the number of additional genes increases because more genes result in more imbalanced protein complexes. Indeed, proliferation rate is negatively correlated with the size of the additional chromosome in $n + 1$ or $2n + 1$ cells (Sheltzer and Amon, 2011; Torres et al., 2007). However, tumor cells usually exhibit karyotypical abnormalities involving many chromosomes (e.g., $2n + x$, where $x > 1$) (Holland and Cleveland, 2009; Weaver and Cleveland, 2006). $2n + x$ cells will contain a mixture of protein complexes balanced at the 2-copy level, complexes that are imbalanced, and complexes balanced at the 3-copy level. Thus, the number of imbalanced protein complexes does not necessarily monotonically increase as the number of additional genes increases in an aneuploid tumor cell. Given this emergent property, new mechanisms that underlie variation in proliferation rate in more complex aneuploid cells may exist. In this study, we used *S. cerevisiae* to generate a variety of $2n + x$ cells and determined how gene copy number affects proliferation.

RESULTS

Proliferation Rate of a $2n + x$ Yeast Strain Is Negatively Correlated with the Total Number of Genes on These x Chromosomes

We first obtained 40 $2n + x$ ($n = 16$) budding yeast strains by collecting the meiotic products of a heterozygous pentaploid strain ($5n$, Figures 1A and S1A). We focused on 10 tetrads in which all 4 meiotic products were viable (Figure 1B). Colony size varied among these strains (Figure 1B). We quantified the area of each colony after a 4-day growth on the tetrad dissection plates and used this to infer the proliferation rate of these $2n + x$ strains.

We performed DNA-seq and obtained the karyotypes of these strains from the single-nucleotide polymorphism (SNP) information (Figure 1C; Table S1). Segregation was independent among each of the 16 chromosomes, and the number of additional chromosomes per strain, x , varied between 5 and 12 in these $2n + x$ strains (Figures 1D, 1E, and S1B). The total number of additional genes varied from 1,764 to 5,376 (Figure 1D) and was negatively correlated with proliferation rate (Figure 1F). Although this negative correlation is consistent with both the balance and the burden hypotheses and with previous findings in $n + 1$ or $2n + 1$ aneuploid cells (Niwa et al., 2006; Sheltzer and Amon, 2011; Torres et al., 2007, 2008, 2010b; Williams et al., 2008), these two hypotheses alone cannot explain the data, as we will explain in the following sections.

The Number of 3-Copy Balanced Protein Complexes ($N_{3\text{-copy}}$) Is Negatively Correlated with Proliferation Rate

We examined the relationship between the status of protein complexes in a $2n + x$ strain and its proliferation rate. We used a manually curated (Pu et al., 2009) set of 408 protein complexes containing 1,617 subunits. In each strain, we defined a protein complex as imbalanced if some subunits of it are encoded by 2 copies of DNA whereas others are encoded by 3 copies; by contrast, a 2- or 3-copy balanced complex has all of its subunits encoded by 2 or 3 copies of DNA (Figure 2A). We counted the number of 2-copy balanced ($N_{2\text{-copy}}$), imbalanced (N_{imb}), and 3-copy balanced ($N_{3\text{-copy}}$) protein complexes, respectively, in each $2n + x$ strain (Figure 2A). The simulation shows that $N_{2\text{-copy}}$ monotonically decreases and $N_{3\text{-copy}}$ monotonically increases as the number of additional chromosomes increases. In contrast, N_{imb} first increases and then decreases (Figure 2B). Because the total of them ($N_{2\text{-copy}} + N_{\text{imb}} + N_{3\text{-copy}}$) is equal to the total number of protein complexes (408), we can draw an equilateral triangle where each dot represents a $2n + x$ strain and the distances to three edges represent the numbers of protein complexes in the above-mentioned three categories (Figure S2A), for the convenience of better illustration. As expected, as the number of additional genes increased, $N_{2\text{-copy}}$ monotonically decreased, and $N_{3\text{-copy}}$ monotonically increased. In contrast, N_{imb} first increased and then decreased (Figures 2C and S2A). Therefore, the properties that affect proliferation in complex aneuploidies may be fundamentally different from those in cells that have gained or lost only a single chromosome.

The balance (or burden) hypothesis predicts a negative correlation between N_{imb} and proliferation rate (Figure 2D). However, such a correlation was not observed ($r = 0.01$, $p = 0.94$, Pearson's correlation, Figure 2E). Notably, the proliferation rate of $2n + x$ strains was negatively correlated with $N_{3\text{-copy}}$ ($r = -0.50$, $p = 1 \times 10^{-3}$, Figure 2E). We therefore speculated that the reduced proliferation rate in $2n + x$ strains with large numbers of 3-copy complexes was partly caused by an increase in dosage of entire and balanced protein complexes (the "overdosage hypothesis") (Figure 2D).

It is worth noting that the negative correlation between $N_{3\text{-copy}}$ and proliferation rate remains after dividing complexes into subgroups. For example, we further classified protein complexes into 4 subcellular localizations and still observed a negative correlation between $N_{3\text{-copy}}$ and proliferation rate in each category ($p < 0.05$, Figure S2B; Table S2), suggesting that this negative relationship is independent of subcellular localizations. In addition, we separated protein complexes into two categories according to whether some subunits of the complex are encoded by genes from the whole genome duplication (WGD). The negative correlation between $N_{3\text{-copy}}$ and proliferation rate remained in both categories (Figure S2C), suggesting that the overdosage of entire protein complexes reduces cell proliferation rate even among the protein complexes that are sensitive to dosage balance (Papp et al., 2003).

To determine if the growth defects are due to hybrid incompatibility between the parental non-isogenic yeast strains, we generated 9 diploid strains, 6 heterozygous and 3 homozygous, and measured their fitness in a competition assay (Figure S3A). We did not observe any difference in fitness between homozygotes and heterozygotes (Figure S3B). Furthermore, we

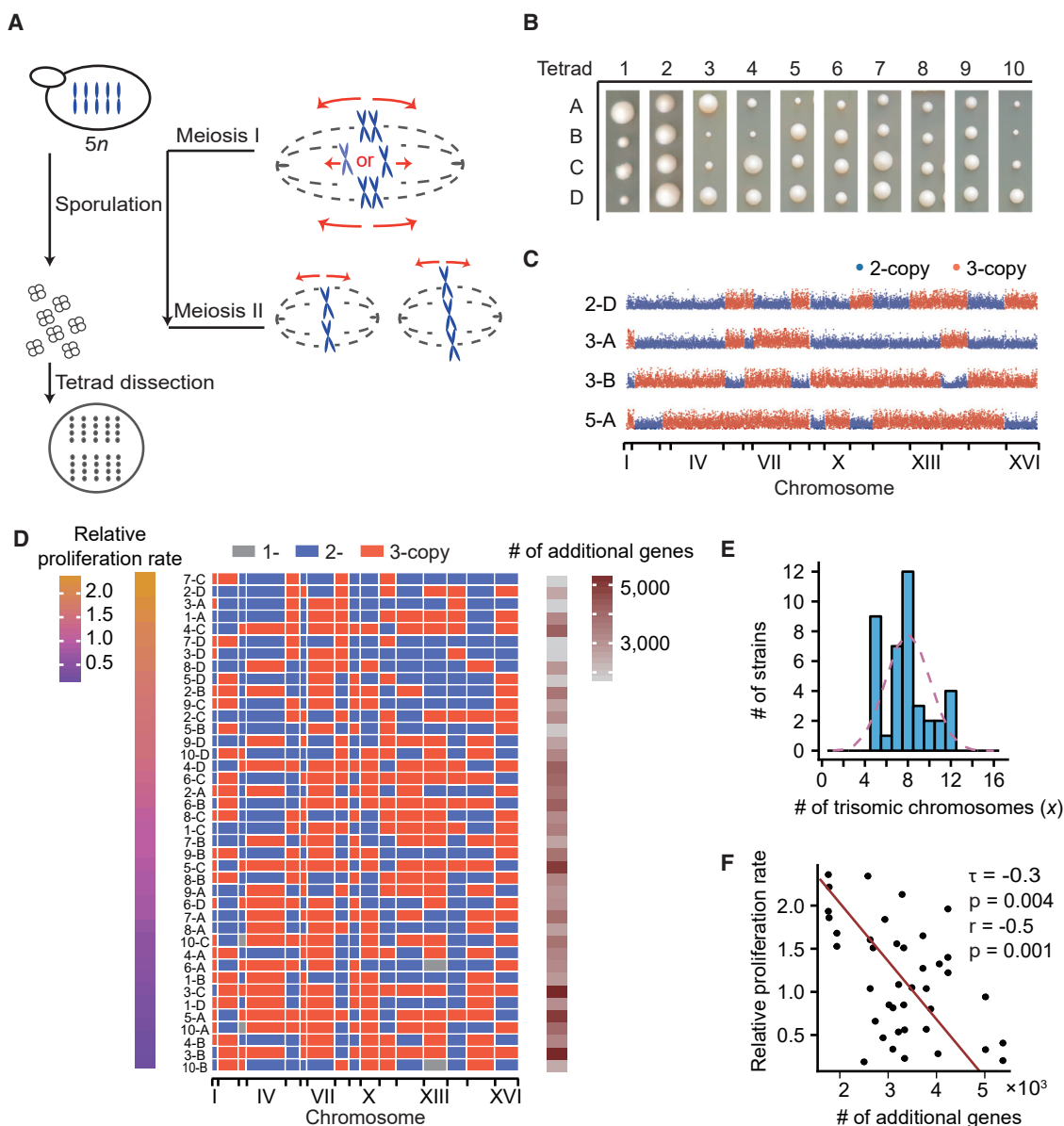


Figure 1. Proliferation Rate Is Negatively Correlated with the Total Number of Additional Genes in 40 $2n + x$ Strains

(A) A schematic description of the construction of $2n + x$ yeast strains. During meiosis I of the $5n$ strain, each chromosome randomly segregated into one of the two nuclei.

(B) Colonies of 40 heterozygous aneuploid strains that were derived from 10 tetrads. Four spores generated in one meiotic event are aligned in one column.

(C) Scatter plots illustrating the karyotypes of 4 heterozygous $2n + x$ strains. Dots show the average sequencing depths of non-overlapping 1,000 bp windows from DNA-seq. 2-copy and 3-copy chromosomes are shown in blue and red, respectively. The 16 chromosomes are concatenated in order along the x axis.

(D) Karyotypes of 40 heterozygous $2n + x$ strains. Strains are ordered by proliferation rate with the number of additional genes in each strain shown in the rightmost column.

(E) The distribution of the number of additional chromosomes (x) among the 40 aneuploid strains. The distribution is indistinguishable from a normal distribution centered at 8 (purple dashed line, $p = 0.61$, one-sample t test).

(F) Proliferation rate is negatively correlated with the number of additional genes, calculated for both Pearson's (r) and Kendall's Tau-a (τ , these symbols represent the respective correlation coefficients in all figures).

See also [Figure S1](#) and [Table S1](#).

generated 52 homozygous $2n + x$ strains by dissecting the meiosis products of a homozygous pentaploid line ([Figures S4A](#) and [S4B](#)), with the number of additional chromosomes varying between 3 and 12 ([Figure S4C](#)), and still observed the

negative correlation between $N_{3\text{-copy}}$ and proliferation rate ([Figure S4D](#)).

$N_{3\text{-copy}}$ is highly correlated with the number of additional genes ($r = 0.94$, [Figure 2C](#)). To determine if the correlation

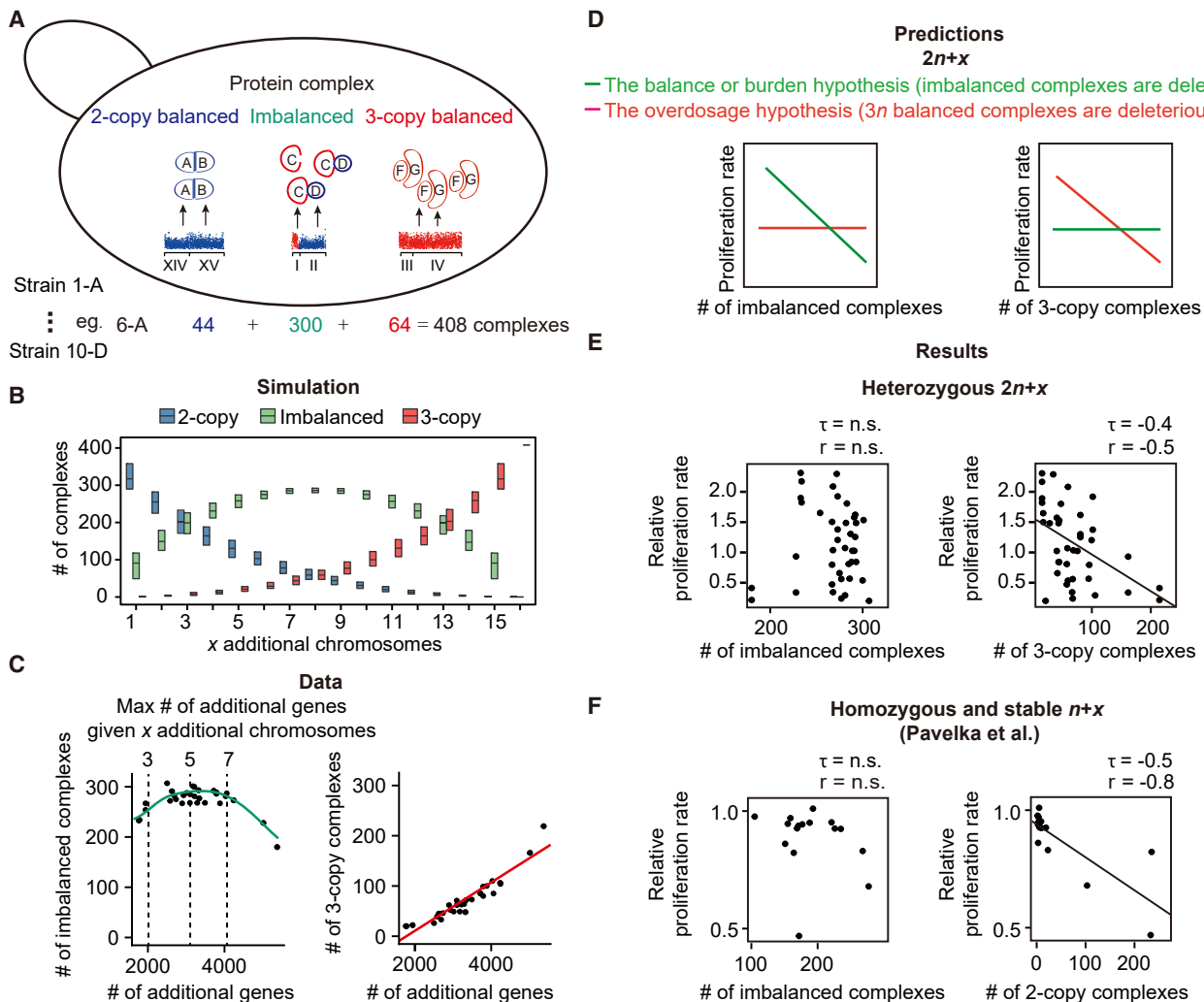


Figure 2. Overdosage of Balanced Protein Complexes Correlates with Reduced Proliferation Rate in Cells with Complex Aneuploidies

(A) In $2n + x$ strains each protein complex can be 2-copy balanced ($N_{2\text{-copy}}$), imbalanced (N_{imb}), or 3-copy balanced ($N_{3\text{-copy}}$). The number of protein complexes in each category is shown for an example strain.

(B) A simulation showing how the number of 2-copy, imbalanced, and 3-copy complexes changes with the number of additional chromosomes. Boxes show the middle 50% of 1,000 simulated strains in which each strain has x random additional chromosomes.

(C) The relationship between the number of additional genes in an aneuploid strain and the number of imbalanced (left) and 3-copy balanced (right) complexes. Each dot represents one heterozygous $2n + x$ strain.

(D) Cartoon showing the expected relation between proliferation rate and the number of additional protein complexes for two models for why aneuploidy causes slow proliferation.

(E and F) Experimental data showing the relation between proliferation rate and the number of additional protein complexes in $2n$ (E) and $1n$ (F) strains with complex aneuploidies. The negative correlations remained after removing 4 outliers in (E) ($r = -0.38$, $p = 0.023$) and 3 outliers in (F) ($r = -0.56$, $p = 0.045$). See also [Figures S2–S5](#) and [Tables S2](#) and [S6](#).

between $N_{3\text{-copy}}$ and proliferation rate is a by-product of the correlation between the number of additional genes and proliferation rate, we further performed a permutation test to investigate the impact of $N_{3\text{-copy}}$ on proliferation rate. We shuffled complex-coding genes and assigned genes into “pseudo” protein complexes, while keeping the total number of complexes and the number of subunits in each complex unchanged. For each set of “pseudo” protein complexes, we calculated the correlation between $N_{3\text{-copy}}$ and proliferation rate. We performed this shuffling 10,000 times and found that the experimentally observed

correlation coefficient between $N_{3\text{-copy}}$ and proliferation rate was significantly stronger than the random expectation based on the number of additional genes ([Figure S4E](#)).

Aneuploid cells often exhibit reduced genomic stability. To control this, we used the read counts from the whole-genome sequencing to calculate the maximum possible fraction of cells with chromosome gains or losses ([Figure S4F](#)). We observed a bimodal distribution; some karyotypes are highly stable and other karyotypes are highly unstable. We defined strains in which less than 10% of cells exhibit intrapopulation karyotype variation

as stable strains (Figure S4G). The negative correlation between $N_{3\text{-copy}}$ and proliferation rate remained only taking into account the stable strains (Figure S4H).

The Number of 2-Copy Balanced Protein Complexes in Homozygous and Stable $n + x$ Yeast Strains Is Negatively Correlated with Proliferation Rate

For a third test of the overdosage hypothesis, we used 16 homozygous and stable $n + x$ haploid yeast strains, each containing an extra copy of any chromosome between 1 to 13 chromosomes (Pavelka et al., 2010). A 2-copy complex in an $n + x$ strain (haploid background) is equivalent to a 3-copy complex in a $2n + x$ strain (diploid background) because in both cases the cell has one extra copy of complexes in addition to the 1- or 2-copy complement (Figure S5). In agreement with the observations in $2n + x$ yeast strains, the number of 2-copy balanced complexes in $n + x$ strains was negatively correlated with proliferation rate ($r = -0.80$, $p = 2 \times 10^{-4}$, Figure 2F), providing additional support for the overdosage hypothesis.

The Additional Subunits of Imbalanced but Not 3-Copy Balanced Protein Complexes Are Degraded in Aneuploid Strains

How can 3-copy balanced protein complexes be deleterious? The unassembled subunits of imbalanced protein complexes are degraded (Dephoure et al., 2014; Gonçalves et al., 2017; Ishikawa et al., 2017; McShane et al., 2016; Ryan et al., 2017; Stingle et al., 2012) (Figure 3A). We speculated that when all subunits of a protein complex are balanced at the 3-copy level, the extra proteins are assembled and less likely to be degraded, leading to an increased protein complex dosage (Figure 3A). This increase may create a stoichiometric imbalance at a higher level, e.g., within a biochemical pathway or signaling pathway, between transcription factors and their DNA targets, etc., and causes the reduction in proliferation rate.

To test this hypothesis, we quantified the transcriptomes and proteomes in nine $2n + x$ strains and in a diploid ($2n$) strain (Figures 3B and 3C). For each $2n + x$ strain, we divided genes into three classes: in an imbalanced protein complex, in a 2-copy balanced protein complex, and in a 3-copy balanced protein complex (Figure 3D). In balanced protein complexes, the majority of 3-copy genes exhibited on average a $3n$ protein level (Figure 3D), consistent with their increase in both DNA and mRNA (Figure S6A). In contrast, in imbalanced protein complexes, the protein concentrations of $\sim 50\%$ of the 3-copy genes were more similar to those of 2-copy genes (Figure 3D), although their mRNA concentrations still exhibited a 0.5-fold increase (Figure S6A).

Examination of two protein complexes showed that when all subunits of a protein complex are balanced at the 3-copy level, the protein levels of these subunits increased (Figures 3E and S6B–S6D). In contrast, the additional subunits in imbalanced protein complexes were specifically degraded (Figures 3E and S6B–S6D). These observations suggest that the DNA copy number increase of all subunits in a protein complex facilitates the escape from surveillance mechanisms that specifically degrade individually overexpressed subunits. This escape leads to the overdosage of the protein complex.

Deleting One Copy of a 3-Copy Balanced Protein Complex Partially Restores Proliferation Rate

To test whether overdosage of a single balanced protein complex can reduce growth rate, we knocked out one copy of each gene in a 3-copy balanced protein complex and determined if proliferation rate was partially restored. To this end, we randomly chose three 2-subunit protein complexes that are balanced at the 3-copy level in a $2n + x$ aneuploid strain: Cdc28p/Clb5p complex, Sgv1p/Bur2p complex, and ISW1a complex. Cdc28p/Clb5p complex regulates mitotic and meiotic cell cycle, Sgv1p/Bur2p complex is involved in the transcriptional regulation, and ISW1a complex has nucleosome-stimulated ATPase activity. For each complex, one copy of one subunit was knocked out with KanMX and GFP, generating an imbalanced variant marked with GFP for the competition assay (Figure 4A). That of the other was further knocked out with NatMX, generating a 2-copy variant. We co-cultured the 2-copy (or imbalanced) and 3-copy variants in rich media and used flow cytometry to measure the relative frequency of each variant over time (Figure 4A).

The balance (or burden) hypothesis predicts that the 2-copy and the 3-copy variants should have the same growth rate, while the imbalanced variant should have a fitness defect (Figure 4B). The overdosage hypothesis predicts that the 2-copy variant should have a higher growth rate than the 3-copy variant because it confers the wild-type concentration of the protein complexes, while the imbalanced and 2-copy variants should have the same growth rate (Figure 4B). Both hypotheses were supported by these experiments on individual complexes (Figure 4C). Each hypothesis alone was not sufficient to explain the fitness of 2-copy, imbalanced, and 3-copy variants (Figure 4C), suggesting that both balance/burden and overdosage hypotheses play a role in explaining the fitness defect in aneuploid cells.

Dosage-Sensitive Protein Complexes Are Enriched in the Cell-Cycle Pathway

To understand why the overdosage of balanced protein complexes is deleterious, we identified individual dosage-sensitive protein complexes that lead to a reduction in proliferation when present in 3 copies. For each complex, each of the 40 $2n + x$ strain can be classified into one of the following three groups (Figure 5A). If all subunits of the complex are at the 2-copy (or 3-copy) level, we classified this strain into group 2 (or group 3). By contrast, if some subunits are at the 2-copy level whereas others are at the 3-copy level, we classified this strain into group i (imbalance). The overdosage hypothesis predicts that the strains in group 3, where the dosage of balanced protein complexes is higher, will exhibit significantly lower proliferation rates than those in group 2 (Figures 5B and S5). We compared the proliferation rates between these two groups of strains for each protein complex and in total identified 123 dosage-sensitive protein complexes ($p < 0.05$, t test, Table S3; Figure S7). Tubulins, as an example, were shown in Figures 5B and S7B.

We retrieved all 387 genes encoding the subunits of these dosage-sensitive protein complexes (Figure 5B). Intriguingly, the only Kyoto Encyclopedia of Genes and Genomes (KEGG) term where these genes were enriched was “cell cycle” (False

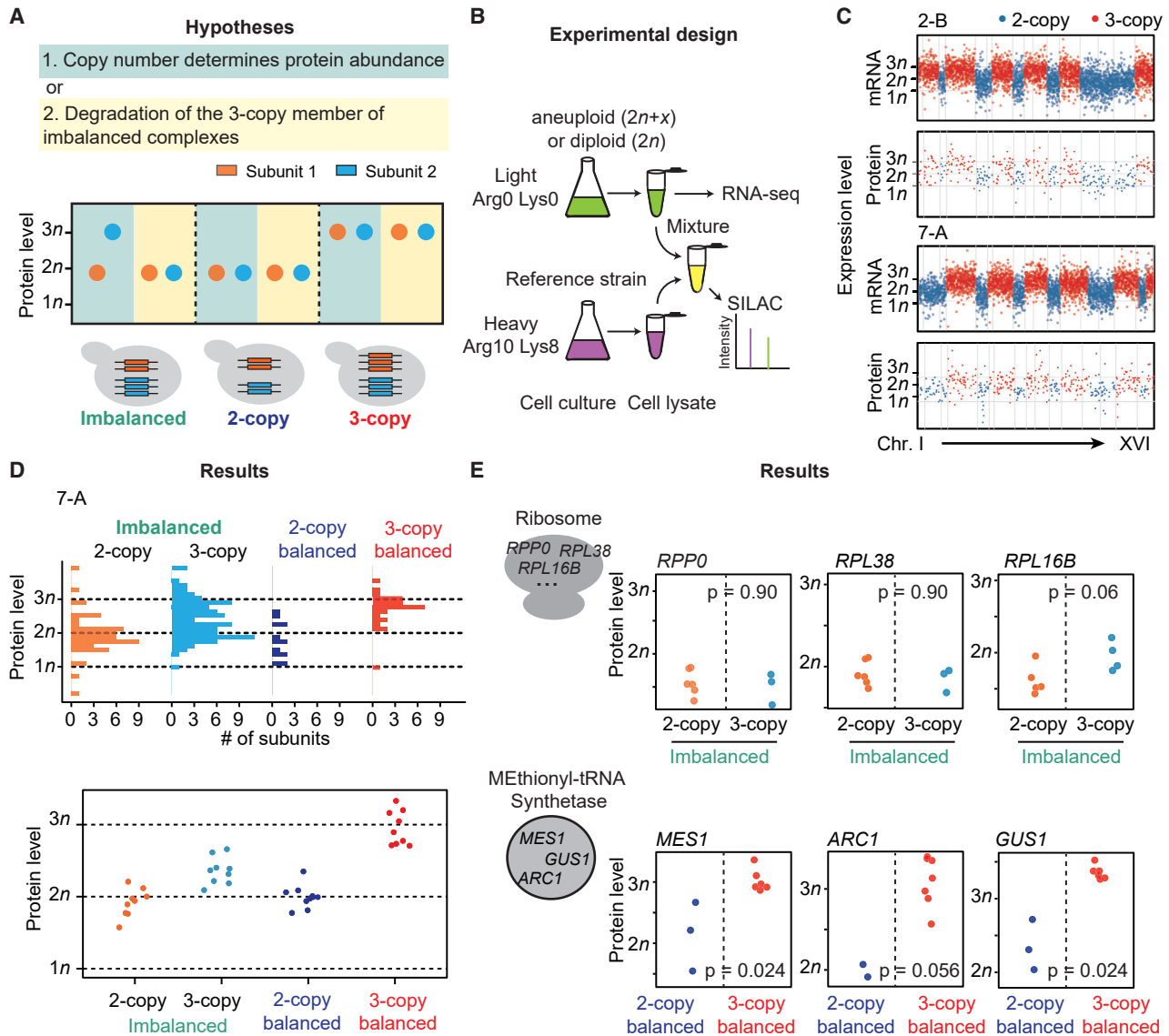


Figure 3. The Subunits of 3-Copy Balanced Protein Complexes Are Not Specifically Degraded in $2n + x$ Strains

(A) The predictions of protein levels of 3-copy subunits in imbalanced and balanced protein complexes.

(B) A schematic illustration of RNA-seq and stable isotope labeling by amino acids in cell culture (SILAC) analysis on nine $2n + x$ strains and a diploid strain.

(C) mRNA and protein abundances largely scale with gene copy numbers (normalized by the diploid strain). Each dot represents one gene. Blue and red dots represent 2-copy and 3-copy genes, respectively. 16 chromosomes are concatenated in order on the x axis.

(D) The measured relative abundance of each protein from each strain, split into imbalanced and balanced classes. The histograms (above) show the distribution of protein levels in heterozygous $2n + x$ strain 7-A. Each dot in the bottom panel shows the average protein level of all proteins belong to the class in one of the nine $2n + x$ strains.

(E) Relative protein abundance of six genes from all 9 strains. Each dot represents the protein level of the gene in one of the nine $2n + x$ strains.

See also Figure S6.

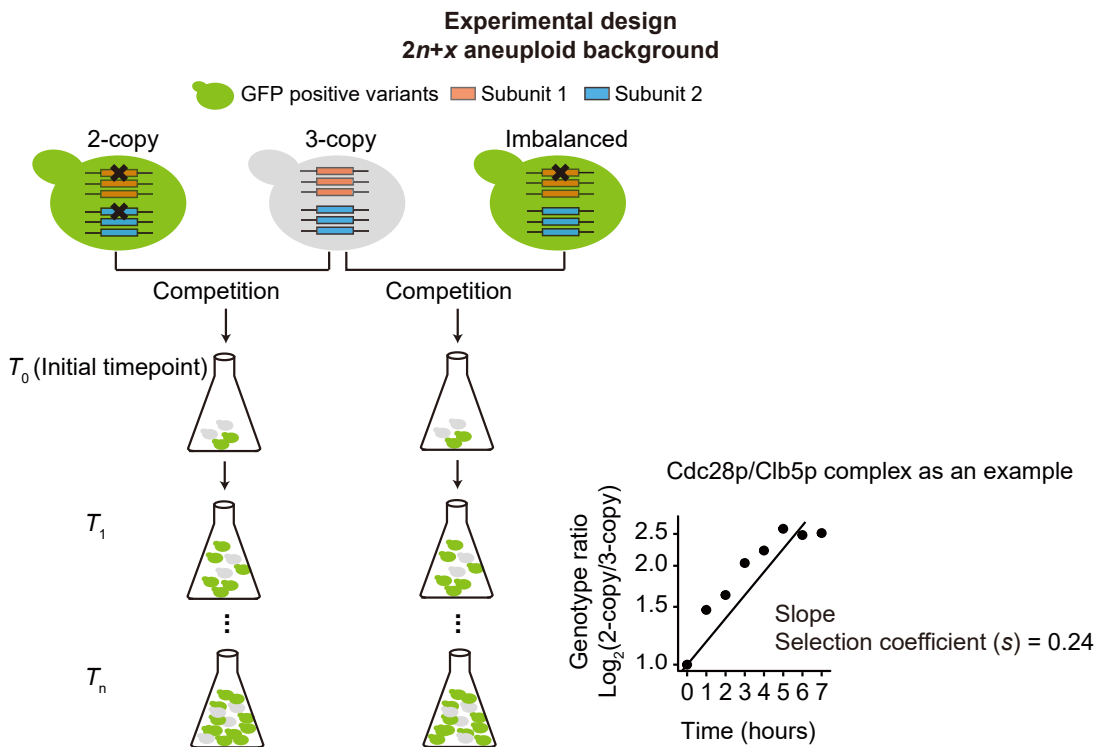
discovery rate, FDR = 0.01, Figure 5C; Table S4). This is in agreement with the previous findings that cell-cycle abnormality was common among aneuploid cells (Beach et al., 2017; Thorburn et al., 2013; Torres et al., 2007). To quantify the cell-cycle defects in these strains, we used Sytox Green staining and flow cytometry to analyze the cell-cycle distribution. We observed that a cell-cycle delay in G_1 stage was negatively correlated with proliferation rate in $2n + x$ cells ($r = -0.71$, $p = 8.7 \times 10^{-4}$, Figures 5D

and 5E), consistent with previous findings that most $n + 1$ yeast strains were delayed in G_1 phase (Torres et al., 2007).

Adding One Copy of a Balanced Protein Complex in the Diploid Background Reduces Proliferation Rate

We further randomly chose 4 additional 2-subunit protein complexes from the set of complexes identified as overdosage sensitive in Table S3, took a homozygous diploid background, and

A

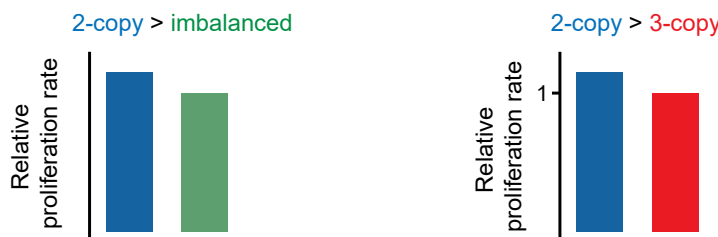


B

Predictions

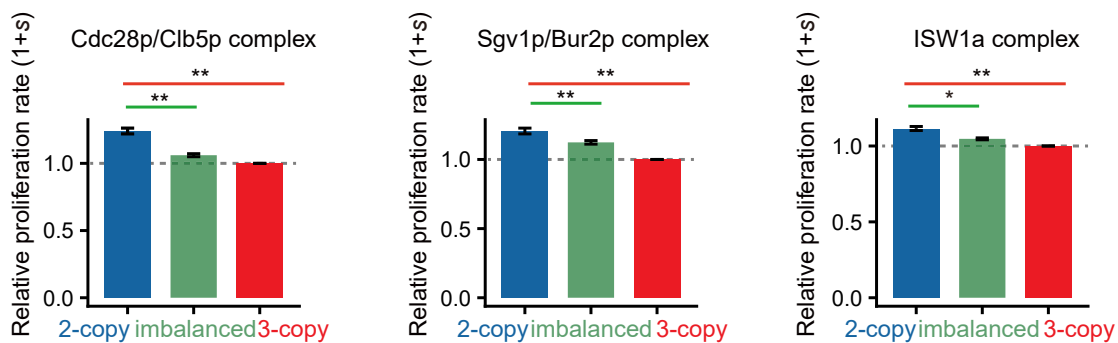
The balance or burden hypothesis
(imbalanced complexes are deleterious)

The overdosage hypothesis
(3n balanced complexes are deleterious)



C

Results



(legend on next page)

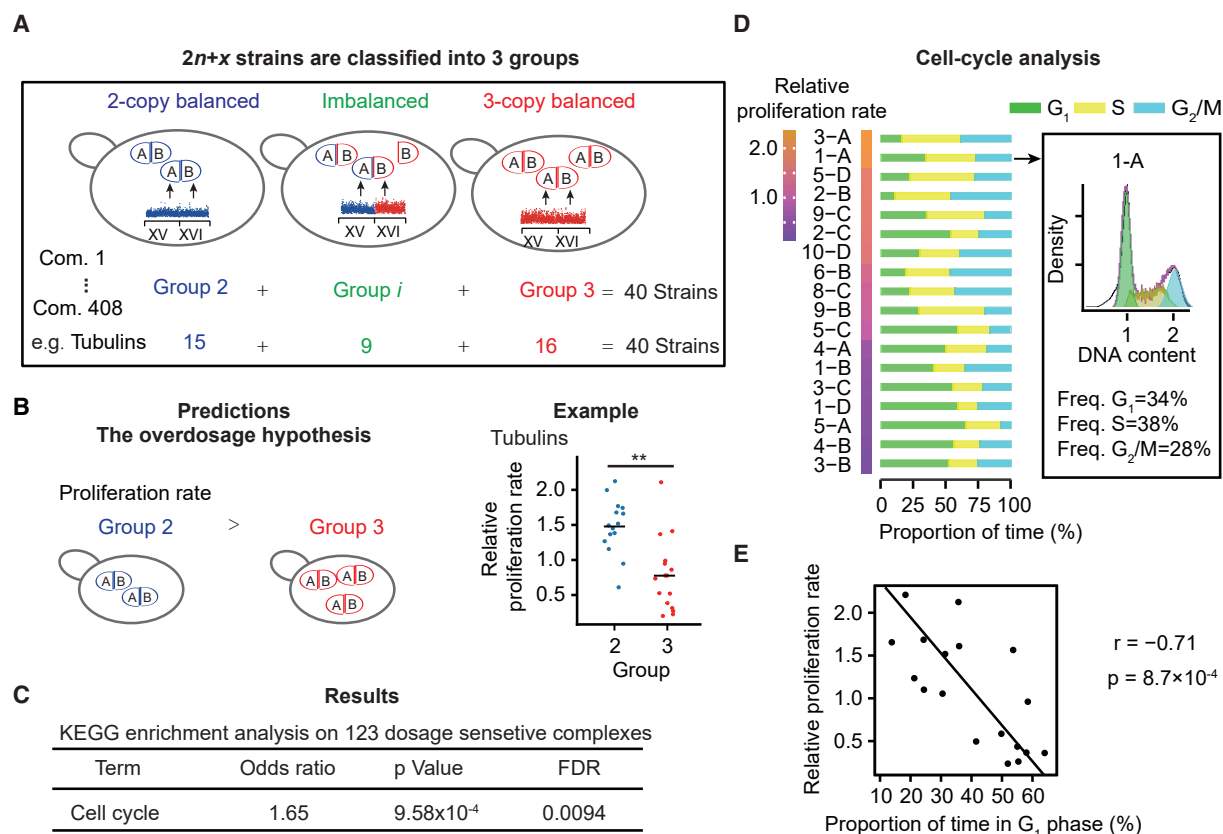


Figure 5. Protein Complexes with Support for the Overdosage Hypothesis Are Enriched in the Cell-Cycle Pathway

(A) For each protein complex, 40 heterozygous $2n + x$ strains were classified into three groups (group 2, group i , and group 3).

(B) The overdosage hypothesis predicts that strains in group 3 proliferating slower than that in group 2. 123 protein complexes are identified in support of the overdosage hypothesis. Tubulins are shown as an example whose dosage is negatively associated with proliferation rate. **, $p < 0.01$.

(C) The results of KEGG enrichment analysis.

(D) $2n + x$ cells exhibit delays at various stages of a cell cycle. The box shows an example how proportion of time in each cell-cycle stage was quantified. Strains are ordered by proliferation rate.

(E) Proliferation rate is negatively correlated with the proportion of time in G_1 stage.

See also [Figures S5 and S7](#) and [Tables S3 and S4](#).

added an extra copy of subunits for each protein complex ([Figure 6A](#)). The balance (or burden) hypothesis predicts that adding one copy of only one subunit of a protein complex should lead to reduced proliferation rate ([Figure 6B](#)), which was observed in two protein complexes ([Figure 6C](#), facilitator of chromatin transcription, FACT, complex and Ubiquitin conjugating enzyme). The overdosage hypothesis predicts that adding one copy of both subunits for a protein complex should lead to reduced growth rate although these protein complexes are stoichiometrically balanced ([Figure 6B](#)). This was observed in three out of the four protein complexes tested ([Figure 6C](#), Bub2p/Bfa1p complex, FACT complex, and Sod1p/Ccs1p complex), indicating

that the overdosage of individual balanced protein complex is sufficient to significantly reduce fitness.

Overdosage of Entire Protein Complexes Is Depleted in Human Cancer Cells

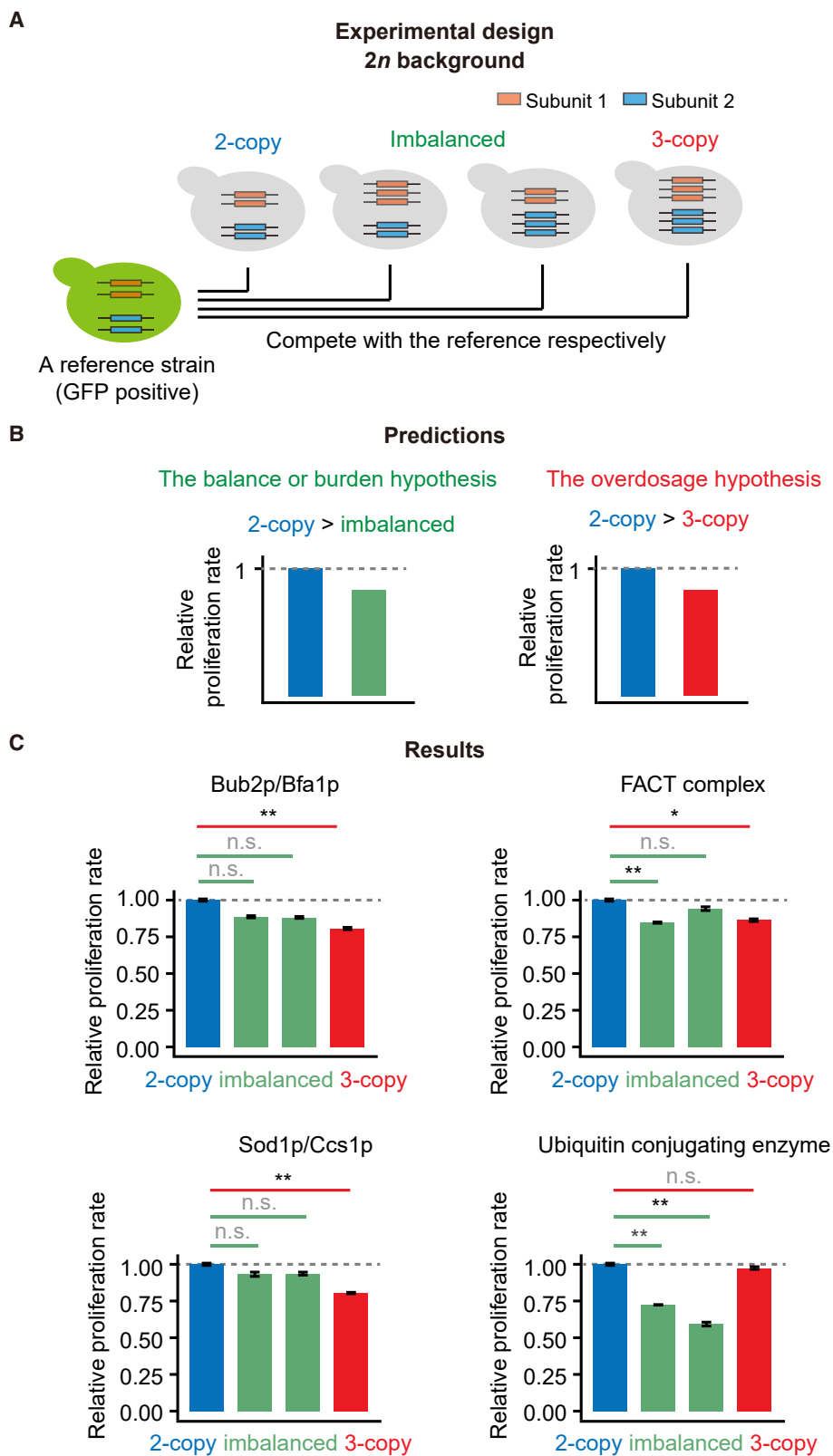
To determine if what holds for yeast cells also applies to human cancer cells, we tested the overdosage hypothesis with copy number variation data from 10,995 cancer samples across 26 cancer types collected in The Cancer Genome Atlas (TCGA) ([Cancer Genome Atlas Research Network et al., 2013](#)). We retrieved the information of 1,521 human protein complexes annotated in the Human Protein Reference Database

Figure 4. Experimental Test of the Balance/Burden and the Overdosage Hypotheses in the $2n + x$ Aneuploid Background

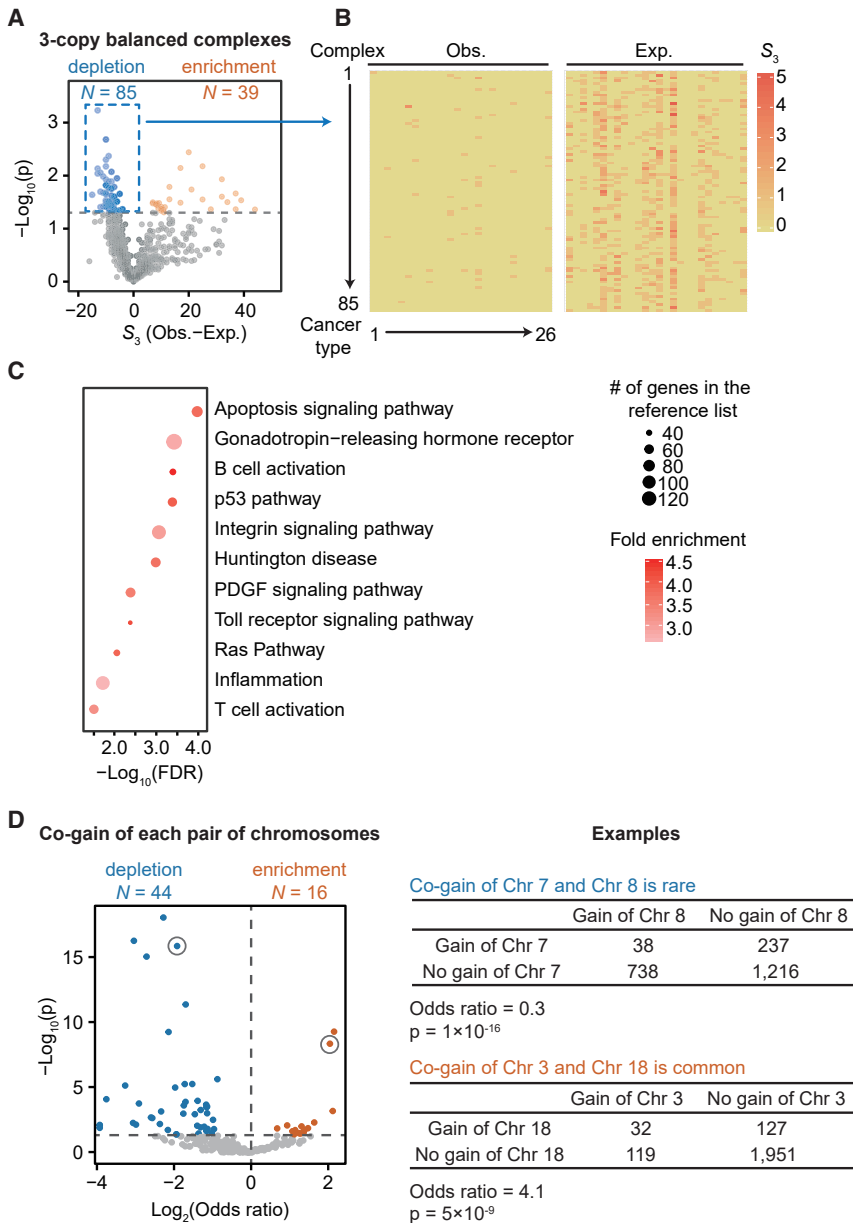
(A) A schematic description of the construction of the 2-copy, 3-copy, and imbalanced variants, and the competition assay. The ratio of population size between 2-copy (or imbalanced, GFP-positive) and 3-copy (GFP-negative) variants was determined by flow cytometry every hour. Taking Cdc28p/Cln5p as an example the selection coefficient is estimated by the slope of the linear regression.

(B) Predictions of the balance/burden and the overdosage hypotheses.

(C) The 2-copy variant shows higher fitness than the imbalanced and the 3-copy variants for each of the three tested complexes. Error bars are the standard errors of proliferation rates. *, $p < 0.05$; **, $p < 0.01$.



(legend on next page)



(Keshava Prasad et al., 2009). For each protein complex and in each cancer type, we counted the number of cancer samples with this complex balanced at the 3-copy level (S_3). As a control, we shuffled the DNA copy numbers of genes encoding subunits of all protein complexes within each cancer sample to obtain the expected S_3 . We identified 85 protein complexes

p53, Figure 7C) that was also identified in yeast, overdosage of protein complexes related to immune reaction was avoided as well. In contrast, significantly less protein complexes exhibited greater observed S_3 (39 versus 85, $p = 4.4 \times 10^{-5}$, binomial test) and these complexes were not enriched in any pathways.

Figure 7. Protein Complexes that Are Avoided to Be Balanced at the 3-Copy Level, and Chromosome Pairs Depleted to Be Co-gained, in Human Cancer Samples

(A) 85 protein complexes (dots in blue) that S_3 are significantly smaller than the random expectation ($p < 0.05$, paired t test, $df = 25$) are identified. S_3 is defined as the number of cancer samples in which the complex is 3-copy balanced. 39 protein complexes (dots in orange) that S_3 are significantly greater than the random expectation are identified. Eight protein complexes exhibited a large difference (Observation - Expectation > 60) in S_3 between the observation and the random expectation because the subunits of them are encoded by genes located on the same chromosomes and are duplicated together; the copy numbers of them tend to change coordinately, and these 8 protein complexes are not shown.

(B) The observed and expected S_3 of the 85 protein complexes identified in (A) in each cancer type.

(C) The result of PANTHER enrichment analysis on the genes encoding these 85 complexes. All genes encoding subunits of human protein complexes were used as the reference.

(D) Chromosome pairs that are enriched and depleted to be co-gained in human cancer samples. Two example 2×2 contingency tables for a pair of chromosomes are shown. Odds ratio > 1 means enrichment of the co-gain of Chr A and Chr B and odds ratio < 1 means depletion of the co-gain of Chr A and Chr B. Sixteen co-gain pairs were found (orange) and 15 out of these pairs were also identified by in Ozwery-Flato et al. More pairs are depleted for co-gains (blue) than are enriched for co-gains ($p = 0.0004$, binomial test).

See also Table S5.

in which the observed S_3 were significantly smaller than the expected S_3 ($p < 0.05$, paired t test, $df = 25$, Figures 7A and 7B; Table S5). The subunits of these 85 complexes were enriched in the pathways inhibiting the proliferation of cancer cells. In addition to the cell-cycle pathway (e.g., apoptosis and

Figure 6. Experimental Test of the Balance/Burden and the Overdosage Hypotheses in a Diploid Background

(A) A schematic description of the construction of the 2-copy, 3-copy, and imbalanced variants, and the competition assay. The ratio of population size between 2-copy (, imbalanced, or 3-copy, GFP-negative) variants and reference strain (GFP-positive, GFP fused with TDH3p, expressed from the chromosome) was determined by flow cytometry every 2 h.

(B) Predictions of the balance/burden and the overdosage hypotheses.

(C) Three out of four tested protein complexes support the overdosage hypothesis (Bub2p/Bfa1p, FACT complex, and Sod1p/Ccs1p). Two protein complexes support the balance (or burden) hypothesis (FACT complex and Ubiquitin conjugating enzyme). Error bars are the standard errors of proliferation rates. *, $p < 0.05$; **, $p < 0.01$.

DISCUSSION

Aneuploid cells have a lower proliferation rate than euploid cells (Birchler and Veitia, 2010; Otto and Whitton, 2000), most likely due to a deviation in the balance of gene copy number (Torres et al., 2008). However, the type of genetic imbalance that causes slow growth remains elusive. Most previous studies focused on imbalance within a protein complex (Papp et al., 2003). A number of studies pointed out that aneuploidy could also lead to other types of imbalance, of the same biochemical pathway or signaling pathway, between transcription factors and their DNA targets (Birchler and Veitia, 2007, 2010, 2012; Veitia, 2004, 2005), etc. However, there was no genome-wide experimental evidence that imbalance, other than that within a protein complex, could result in a growth defect. In this study, we provide the evidence for the importance of dosage balance beyond that within a protein complex.

In this study, we explicitly tested for the support of the balance (or burden) hypothesis as an overall determinant of proliferation rate and for each complex independently. We did find some protein complexes support the balance hypothesis that copy-number imbalance of subunits within individual protein complexes results a proliferation defect (76 out of 408 protein complexes, Table S3 and Figure S7A). Therefore, both the balance/burden and overdosage cause reduced proliferation rates in aneuploid cells; some protein complexes behave according to the overdosage hypothesis, some according to the balance/burden hypothesis, and some according to both. There are at least four possible reasons why the genomic-scale imbalance (N_{imb}) does not correlate with proliferation in our data (Figures 2E and 2F). First, $\sim 34\%$ of $2n + x$ spores did not grow up to form colonies, which may be because of the fact that severe imbalance within some protein complexes was lethal. Spores that did not form colonies were not included in this study. Second, mechanisms exist whose end result is that an increase in gene copy-number of a single subunit does not lead to an increase in protein levels (Birchler and Veitia, 2012; Dephoure et al., 2014; Ishikawa et al., 2017; McShane et al., 2016; Stingle et al., 2012); over 50% of subunits present in 3 copies in imbalanced complexes were expressed at the 2-copy level in the proteome (Figure 3). A third possible reason for the lack of correlation between the number of imbalanced protein complexes (N_{imb}) and proliferation rate is additional effects from other factors, namely the total number of additional genes and the number of 3-copy balanced complexes (N_{3-copy}). Indeed, a linear model that predicts proliferation rate of 40 heterozygous $2n + x$ strains from all three parameters: the number of additional genes, N_{imb} , and N_{3-copy} , performs better (akaike information criterion, AIC = 60) than models that include the number of additional genes plus one of the other two parameters (AIC = 68.5 after removing N_{3-copy} and 71.7 after removing N_{imb}). A similar pattern was also observed among the 16 $n + x$ and 52 homozygous $2n + x$ strains (Table S6). Therefore, both the balance/burden and the overdosage hypotheses are supported by our data. Lastly, “bridge” subunits (Bray and Lay, 1997) play a central role in the assembly of protein complexes and are likely more sensitive to stoichiometric imbalance. However, such bridge subunits have not been identified genome widely. The effect of

the imbalance of such subunits may be masked by a large number of other subunits that are not sensitive to stoichiometric imbalance.

The overdosage model predicts that co-gain or co-loss of certain combinations of chromosomes should be avoided, as they will produce overdosage of balanced protein complexes. In contrast, the balance/burden hypothesis predicts that pairs of chromosomes should be co-gained or co-lost to avoid generating imbalanced complexes. Using karyotypes in the Mitelman database of chromosome aberrations and gene fusions in cancer (<http://cgap.nci.nih.gov/Chromosomes/Mitelman>), Ozery-Flato et al. found significant support for co-gain and co-loss of chromosome pairs in cancer (Ozery-Flato et al., 2011), in support of the balance/burden hypothesis. We reanalyzed the data from the Mitelman database, used the cells with 48 chromosomes (46 + two additional, + Chr A + Chr B), and asked if chromosomes A and B are gained independently by Fisher’s exact test. Consistent with Ozery-Flato et al., we found significant support for co-gains. However, the avoidance of the co-gain of specific pairs of chromosomes is more common (44 versus 16, $p = 4 \times 10^{-4}$, binomial test, Figure 7D), in support of the overdosage hypothesis.

Protein complexes that are avoided to be balanced at the 3-copy level in human cancer samples were enriched in a number of pathways (Figure 7C). Some of these signaling pathways seem to promote tumorigenesis (e.g., Ras pathway), which is not expected. However, a careful inspection revealed that the overexpression of part of such pathways might actually suppress the proliferation of cancer cells. For example, 3 proteins (KSR1, EPHB2, and MAP2K1) in the Ras pathway form a protein complex and this complex was not balanced at the 3-copy level in any of the 10,995 cancer samples examined ($p = 0.02$, Table S5), likely because Kinase Suppressor of Ras (KSR1) suppresses tumorigenesis through forming a protein complex with the other two proteins (Denouel-Galy et al., 1998; Yu et al., 1998). This is consistent with our hypothesis that the overdosage of an entire protein complex causes the stoichiometric imbalance at a higher level, such as in a signaling pathway. In addition, some other pathways (e.g., Huntington disease) seem to be unrelated to tumorigenesis. However, patients with Huntington disease actually exhibited a lower cancer risk (Sørensen et al., 1999), probably due to the role of expanded polyglutamine in stimulating p53 pathway (Bae et al., 2005).

In the tumor data, it is difficult to disentangle proliferation from viability. Cancer cells with complex aneuploidies that result in very low proliferation rates are unlikely to form clinically relevant tumors and therefore will be unobserved in tumor data. However, we can infer inviable yeast genotypes from the frequency of genotypes of viable spores in tetrads. Specifically, we can count the strains with 2-copy, imbalanced, and 3-copy balanced complexes for each protein complex. If all spores are viable, the number of these strains should follow a binomial distribution (i.e., 10, 20, and 10 among the 40 heterozygous $2n + x$ strains, respectively, for a 2-subunit complex). For tubulins, the numbers of strains in these three groups were 15, 9, and 16, respectively (Figure S7C), and viable spores with imbalanced tubulins were less abundant than the random expectation ($p = 3 \times 10^{-4}$, G test), suggesting that imbalanced tubulin reduces viability. Therefore, yeast, where viability and proliferation can be analyzed independently, is a promising system for the future determination if inviable karyotypes are similar to those with

very low proliferation rates, or if the karyotypes that lead to inviability are categorically different from those that result in low fitness.

STAR★METHODS

Detailed methods are provided in the online version of this paper and include the following:

- **KEY RESOURCES TABLE**
- **LEAD CONTACT AND MATERIALS AVAILABILITY**
 - Materials Availability Statement
- **METHOD DETAILS**
 - Construction of Heterozygous $2n+x$ Strains
 - Construction of Homozygous $2n+x$ Strains
 - Construction of Variants in a $2n+x$ Background
 - Construction of Variants in a $2n$ Background
 - DNA Sequencing
 - mRNA Sequencing
 - SILAC
 - DNA Content Analysis Using Flow Cytometry
- **QUANTIFICATION AND STATISTICAL ANALYSIS**
 - Quantifying Proliferation Rate
 - Karyotyping Heterozygous $2n+x$ Aneuploidies
 - Karyotyping Homozygous $2n+x$ Aneuploidies
 - Calculating Subcolonial Karyotype Variation
 - Quantifying mRNA Abundance
 - Quantifying Protein Abundance
 - Estimating Relative Time in Cell-Cycle Stages
 - Data Retrieval
- **DATA AND CODE AVAILABILITY**

SUPPLEMENTAL INFORMATION

Supplemental Information can be found online at <https://doi.org/10.1016/j.cels.2019.06.007>.

ACKNOWLEDGMENTS

We thank Calum Maclean for providing yeast strains. We thank Xiaolei Su, Ye Tian, and Jianzhi Zhang for discussion and James A. Birchler, Xionglei He, and Jian-Rong Yang for critical comments on the manuscript. This work was supported by grants from National Natural Science Foundation of China to W.Q. (91731302). L.B.C. was supported by grants from the Ministerio de Economía y Competitividad (MINECO) (BFU2015-68351-P) and AGAUR (2014SGR0974 and 2017SGR1054) and the Unidad de Excelencia María de Maeztu, funded by the MINECO (MDM-2014-0370).

AUTHOR CONTRIBUTIONS

Y.C. and W.Q. conceived the research; Y.C., S.C., K.L., X.H., T.L., and Y.W. performed the experiments; Y.C. and Y.Z. analyzed the data; Y.C., S.W., L.B.C., and W.Q. wrote the manuscript.

DECLARATION OF INTERESTS

The authors declare no competing interests.

Received: July 24, 2018
 Revised: February 27, 2019
 Accepted: June 17, 2019
 Published: July 24, 2019

WEB RESOURCES

Mitelman Database of Chromosome Aberrations and Gene Fusions in Cancer, <http://cgap.nci.nih.gov/Chromosomes/Mitelman>

REFERENCES

- Abovich, N., Gritz, L., Tung, L., and Rosbash, M. (1985). Effect of RP51 gene dosage alterations on ribosome synthesis in *Saccharomyces cerevisiae*. *Mol. Cell. Biol.* 5, 3429–3435.
- Abruzzi, K.C., Smith, A., Chen, W., and Solomon, F. (2002). Protection from free beta-tubulin by the beta-tubulin binding protein Rbl2p. *Mol. Cell. Biol.* 22, 138–147.
- Agrawal, M.G., and Bowman, L.H. (1987). Transcriptional and translational regulation of ribosomal protein formation during mouse myoblast differentiation. *J. Biol. Chem.* 262, 4868–4875.
- Albertson, D.G., Collins, C., McCormick, F., and Gray, J.W. (2003). Chromosome aberrations in solid tumors. *Nat. Genet.* 34, 369–376.
- Bae, B.I., Xu, H., Igarashi, S., Fujimuro, M., Agrawal, N., Taya, Y., Hayward, S.D., Moran, T.H., Montell, C., Ross, C.A., et al. (2005). p53 mediates cellular dysfunction and behavioral abnormalities in Huntington's disease. *Neuron* 47, 29–41.
- Bahler, J., Wu, J.Q., Longtine, M.S., Shah, N.G., McKenzie, A., 3rd, Steever, A.B., Wach, A., Philippsen, P., and Pringle, J.R. (1998). Heterologous modules for efficient and versatile PCR-based gene targeting in *Schizosaccharomyces pombe*. *Yeast* 14, 943–951.
- Baker, D.J., Jeganathan, K.B., Cameron, J.D., Thompson, M., Juneja, S., Kopecka, A., Kumar, R., Jenkins, R.B., de Groen, P.C., Roche, P., et al. (2004). BubR1 insufficiency causes early onset of aging-associated phenotypes and infertility in mice. *Nat. Genet.* 36, 744–749.
- Beach, R.R., Ricci-Tam, C., Brennan, C.M., Moomau, C.A., Hsu, P.H., Hua, B., Silberman, R.E., Springer, M., and Amon, A. (2017). Aneuploidy causes non-genetic individuality. *Cell* 169, 229–242.
- Birchler, J.A., and Veitia, R.A. (2007). The gene balance hypothesis: from classical genetics to modern genomics. *Plant Cell* 19, 395–402.
- Birchler, J.A., and Veitia, R.A. (2010). The gene balance hypothesis: implications for gene regulation, quantitative traits and evolution. *New Phytol.* 186, 54–62.
- Birchler, J.A., and Veitia, R.A. (2012). Gene balance hypothesis: connecting issues of dosage sensitivity across biological disciplines. *Proc. Natl. Acad. Sci. USA* 109, 14746–14753.
- Brachmann, C.B., Davies, A., Cost, G.J., Caputo, E., Li, J., Hieter, P., and Boeke, J.D. (1998). Designer deletion strains derived from *Saccharomyces cerevisiae* S288C: a useful set of strains and plasmids for PCR-mediated gene disruption and other applications. *Yeast* 14, 115–132.
- Bray, D., and Lay, S. (1997). Computer-based analysis of the binding steps in protein complex formation. *Proc. Natl. Acad. Sci. USA* 94, 13493–13498.
- Cancer Genome Atlas Research Network, Weinstein, J.N., Collisson, E.A., Mills, G.B., Shaw, K.R., Ozenberger, B.A., Ellrott, K., Shmulevich, I., Sander, C., and Stuart, J.M. (2013). The Cancer Genome Atlas Pan-Cancer analysis project. *Nat. Genet.* 45, 1113–1120.
- Cherry, J.M., Hong, E.L., Amundsen, C., Balakrishnan, R., Binkley, G., Chan, E.T., Christie, K.R., Costanzo, M.C., Dwight, S.S., Engel, S.R., et al. (2012). *Saccharomyces Genome Database: the genomics resource of budding yeast*. *Nucleic Acids Res.* 40, D700–D705.
- Cox, J., Matic, I., Hilger, M., Nagaraj, N., Selbach, M., Olsen, J.V., and Mann, M. (2009). A practical guide to the MaxQuant computational platform for SILAC-based quantitative proteomics. *Nat. Protoc.* 4, 698–705.
- de Godoy, L.M., Olsen, J.V., Cox, J., Nielsen, M.L., Hubner, N.C., Fröhlich, F., Walther, T.C., and Mann, M. (2008). Comprehensive mass-spectrometry-based proteome quantification of haploid versus diploid yeast. *Nature* 455, 1251–1254.

- Denouel-Galy, A., Douville, E.M., Warne, P.H., Papin, C., Laugier, D., Calothy, G., Downward, J., and Eychène, A. (1998). Murine Ksr interacts with MEK and inhibits Ras-induced transformation. *Curr. Biol.* **8**, 46–55.
- Dephoure, N., Hwang, S., O'Sullivan, C., Dodgson, S.E., Gygi, S.P., Amon, A., and Torres, E.M. (2014). Quantitative proteomic analysis reveals posttranslational responses to aneuploidy in yeast. *Elife* **3**, e03023.
- eIbaradi, T.T., van der Sande, C.A., Mager, W.H., Raué, H.A., and Planta, R.J. (1986). The cellular level of yeast ribosomal protein L25 is controlled principally by rapid degradation of excess protein. *Curr. Genet.* **10**, 733–739.
- Geiler-Samerotte, K.A., Dion, M.F., Budnik, B.A., Wang, S.M., Hartl, D.L., and Drummond, D.A. (2011). Misfolded proteins impose a dosage-dependent fitness cost and trigger a cytosolic unfolded protein response in yeast. *Proc. Natl. Acad. Sci. USA* **108**, 680–685.
- Goldstein, A.L., and McCusker, J.H. (1999). Three new dominant drug resistance cassettes for gene disruption in *Saccharomyces cerevisiae*. *Yeast* **15**, 1541–1553.
- Gonçalves, E., Fragoulis, A., Garcia-Alonso, L., Cramer, T., Saez-Rodriguez, J., and Beltrao, P. (2017). Widespread post-transcriptional attenuation of genomic copy-number variation in cancer. *Cell Syst.* **5**, 386–398.
- Gunjan, A., and Verreault, A. (2003). A Rad53 kinase-dependent surveillance mechanism that regulates histone protein levels in *S. cerevisiae*. *Cell* **115**, 537–549.
- Holland, A.J., and Cleveland, D.W. (2009). Boveri revisited: chromosomal instability, aneuploidy and tumorigenesis. *Nat. Rev. Mol. Cell Biol.* **10**, 478–487.
- Ishikawa, K., Makanae, K., Iwasaki, S., Ingolia, N.T., and Moriya, H. (2017). Post-translational dosage compensation buffers genetic perturbations to stoichiometry of protein complexes. *PLoS Genet.* **13**, e1006554.
- Katz, W., Weinstein, B., and Solomon, F. (1990). Regulation of tubulin levels and microtubule assembly in *Saccharomyces cerevisiae*: consequences of altered tubulin gene copy number. *Mol. Cell. Biol.* **10**, 5286–5294.
- Kellis, M., Birren, B.W., and Lander, E.S. (2004). Proof and evolutionary analysis of ancient genome duplication in the yeast *Saccharomyces cerevisiae*. *Nature* **428**, 617–624.
- Keshava Prasad, T.S., Goel, R., Kandasamy, K., Keerthikumar, S., Kumar, S., Mathivanan, S., Telikicherla, D., Raju, R., Shafreen, B., Venugopal, A., et al. (2009). Human Protein Reference Database–2009 update. *Nucleic Acids Res.* **37**, D767–D772.
- Langmead, B., and Salzberg, S.L. (2012). Fast gapped-read alignment with Bowtie 2. *Nat. Methods* **9**, 357–359.
- Li, H., and Durbin, R. (2009). Fast and accurate short read alignment with Burrows-Wheeler transform. *Bioinformatics* **25**, 1754–1760.
- Li, H., Handsaker, B., Wysoker, A., Fennell, T., Ruan, J., Homer, N., Marth, G., Abecasis, G., Durbin, R., and Genome Project Data Processing, S. (2009). The Sequence Alignment/Map format and SAMtools. *Bioinformatics* **25**, 2078–2079.
- Li, H. (2011). A statistical framework for SNP calling, mutation discovery, association mapping and population genetical parameter estimation from sequencing data. *Bioinformatics* **27**, 2987–2993.
- Loidl, J. (1995). Meiotic chromosome pairing in triploid and tetraploid *Saccharomyces cerevisiae*. *Genetics* **139**, 1511–1520.
- Maclean, C.J., Metzger, B.P.H., Yang, J.R., Ho, W.C., Moyers, B., and Zhang, J. (2017). Deciphering the Genic Basis of Yeast Fitness Variation by Simultaneous Forward and Reverse Genetics. *Mol. Biol. Evol.* **34**, 2486–2502.
- Maicas, E., Pluthero, F.G., and Friesen, J.D. (1988). The accumulation of three yeast ribosomal proteins under conditions of excess mRNA is determined primarily by fast protein decay. *Mol. Cell. Biol.* **8**, 169–175.
- McKenna, A., Hanna, M., Banks, E., Sivachenko, A., Cibulskis, K., Kernysky, A., Garimella, K., Altshuler, D., Gabriel, S., Daly, M., et al. (2010). The Genome Analysis Toolkit: a MapReduce framework for analyzing next-generation DNA sequencing data. *Genome Res.* **20**, 1297–1303.
- McShane, E., Sin, C., Zaubner, H., Wells, J.N., Donnelly, N., Wang, X., Hou, J., Chen, W., Storchova, Z., Marsh, J.A., et al. (2016). Kinetic analysis of protein stability reveals age-dependent degradation. *Cell* **167**, 803–815.
- Niwa, O., Tange, Y., and Kurabayashi, A. (2006). Growth arrest and chromosome instability in aneuploid yeast. *Yeast* **23**, 937–950.
- Niwa, O., and Yanagida, M. (1985). Triploid meiosis and aneuploidy in *Schizosaccharomyces pombe* - an unstable aneuploid disomic for Chromosome-III. *Curr. Genet.* **9**, 463–470.
- Oromendia, A.B., and Amon, A. (2014). Aneuploidy: implications for protein homeostasis and disease. *Dis. Models Mech.* **7**, 15–20.
- Oromendia, A.B., Dodgson, S.E., and Amon, A. (2012). Aneuploidy causes proteotoxic stress in yeast. *Genes Dev.* **26**, 2696–2708.
- Otto, S.P., and Whitton, J. (2000). Polyploid incidence and evolution. *Annu. Rev. Genet.* **34**, 401–437.
- Ozery-Flato, M., Linhart, C., Trakhtenbrot, L., Izraeli, S., and Shamir, R. (2011). Large-scale analysis of chromosomal aberrations in cancer karyotypes reveals two distinct paths to aneuploidy. *Genome Biol.* **12**, R61.
- Papp, B., Pál, C., and Hurst, L.D. (2003). Dosage sensitivity and the evolution of gene families in yeast. *Nature* **424**, 194–197.
- Parry, E.M., and Cox, B.S. (1970). The tolerance of aneuploidy in yeast. *Genet. Res.* **16**, 333–340.
- Pavelka, N., Rancati, G., Zhu, J., Bradford, W.D., Saraf, A., Florens, L., Sanderson, B.W., Hattam, G.L., and Li, R. (2010). Aneuploidy confers quantitative proteome changes and phenotypic variation in budding yeast. *Nature* **468**, 321–325.
- Pu, S., Wong, J., Turner, B., Cho, E., and Wodak, S.J. (2009). Up-to-date catalogues of yeast protein complexes. *Nucleic Acids Res.* **37**, 825–831.
- Qian, W., Ma, D., Xiao, C., Wang, Z., and Zhang, J. (2012). The genomic landscape and evolutionary resolution of antagonistic pleiotropy in yeast. *Cell Rep.* **2**, 1399–1410.
- Ryan, C.J., Kennedy, S., Bajrami, I., Matallanas, D., and Lord, C.J. (2017). A compendium of co-regulated protein complexes in breast cancer reveals collateral loss events. *Cell Syst.* **5**, 399–409.
- Segal, D.J., and McCoy, E.E. (1974). Studies on Down's syndrome in tissue culture. I. Growth rates and protein contents of fibroblast cultures. *J. Cell. Physiol.* **83**, 85–90.
- Sheltzer, J.M., and Amon, A. (2011). The aneuploidy paradox: costs and benefits of an incorrect karyotype. *Trends Genet.* **27**, 446–453.
- Sheltzer, J.M., Blank, H.M., Pfau, S.J., Tange, Y., George, B.M., Humpton, T.J., Brito, I.L., Hiraoka, Y., Niwa, O., and Amon, A. (2011). Aneuploidy drives genomic instability in yeast. *Science* **333**, 1026–1030.
- Sheltzer, J.M., Ko, J.H., Replogle, J.M., Habibe Burgos, N.C., Chung, E.S., Meehl, C.M., Sayles, N.M., Passerini, V., Storchova, Z., and Amon, A. (2017). Single-chromosome gains commonly function as tumor suppressors. *Cancer Cell* **31**, 240–255.
- Siegel, J.J., and Amon, A. (2012). New insights into the troubles of aneuploidy. *Annu. Rev. Cell Dev. Biol.* **28**, 189–214.
- Sørensen, S.A., Fenger, K., and Olsen, J.H. (1999). Significantly lower incidence of cancer among patients with Huntington disease: an apoptotic effect of an expanded polyglutamine tract? *Cancer* **86**, 1342–1346.
- Stingele, S., Stoehr, G., Peplowska, K., Cox, J., Mann, M., and Storchova, Z. (2012). Global analysis of genome, transcriptome and proteome reveals the response to aneuploidy in human cells. *Mol. Syst. Biol.* **8**, 608.
- Täckholm, G. (1922). *Zytologische Studien über die Gattung Rosa (Almqvist & Wiksell)*.
- Thompson, S.L., and Compton, D.A. (2008). Examining the link between chromosomal instability and aneuploidy in human cells. *J. Cell Biol.* **180**, 665–672.
- Thorburn, R.R., Gonzalez, C., Brar, G.A., Christen, S., Carlile, T.M., Ingolia, N.T., Sauer, U., Weissman, J.S., and Amon, A. (2013). Aneuploid yeast strains exhibit defects in cell growth and passage through START. *Mol. Biol. Cell* **24**, 1274–1289.
- Torres, E.M., Dephoure, N., Panneerselvam, A., Tucker, C.M., Whittaker, C.A., Gygi, S.P., Dunham, M.J., and Amon, A. (2010a). Identification of aneuploidy-tolerating mutations. *Cell* **143**, 71–83.

- Torres, E.M., Sokolsky, T., Tucker, C.M., Chan, L.Y., Boselli, M., Dunham, M.J., and Amon, A. (2007). Effects of aneuploidy on cellular physiology and cell division in haploid yeast. *Science* *317*, 916–924.
- Torres, E.M., Williams, B.R., and Amon, A. (2008). Aneuploidy: cells losing their balance. *Genetics* *179*, 737–746.
- Torres, E.M., Williams, B.R., Tang, Y.-C., and Amon, A. (2010b). Thoughts on aneuploidy. *Cold Spring Harb. Symp. Quant. Biol.* *75*, 445–451.
- Veitia, R.A. (2002). Exploring the etiology of haploinsufficiency. *BioEssays* *24*, 175–184.
- Veitia, R.A. (2004). Gene dosage balance in cellular pathways: implications for dominance and gene duplicability. *Genetics* *168*, 569–574.
- Veitia, R.A. (2005). Gene dosage balance: deletions, duplications and dominance. *Trends Genet.* *21*, 33–35.
- Vizcaino, J.A., Côté, R.G., Csordas, A., Dienes, J.A., Fabregat, A., Foster, J.M., Griss, J., Alpi, E., Birim, M., Contell, J., et al. (2013). The Proteomics Identifications (PRIDE) database and associated tools: status in 2013. *Nucleic Acids Res.* *41*, D1063–D1069.
- Wang, Y., Song, F., Zhu, J., Zhang, S., Yang, Y., Chen, T., Tang, B., Dong, L., Ding, N., Zhang, Q., et al. (2017). GSA: genome sequence archive. *Genomics Proteomics Bioinformatics* *15*, 14–18.
- Warner, J.R., Mitra, G., Schwindinger, W.F., Studeny, M., and Fried, H.M. (1985). *Saccharomyces cerevisiae* coordinates accumulation of yeast ribosomal proteins by modulating mRNA splicing, translational initiation, and protein turnover. *Mol. Cell. Biol.* *5*, 1512–1521.
- Weaver, B.A., and Cleveland, D.W. (2006). Does aneuploidy cause cancer? *Curr. Opin. Cell Biol.* *18*, 658–667.
- Whitesell, L., and Lindquist, S.L. (2005). HSP90 and the chaperoning of cancer. *Nat. Rev. Cancer* *5*, 761–772.
- Williams, B.R., Prabhu, V.R., Hunter, K.E., Glazier, C.M., Whittaker, C.A., Housman, D.E., and Amon, A. (2008). Aneuploidy affects proliferation and spontaneous immortalization in mammalian cells. *Science* *322*, 703–709.
- Yu, W., Fantl, W.J., Harrowe, G., and Williams, L.T. (1998). Regulation of the MAP kinase pathway by mammalian Ksr through direct interaction with MEK and ERK. *Curr. Biol.* *8*, 56–64.

STAR★METHODS

KEY RESOURCES TABLE

REAGENT or RESOURCE	SOURCE	IDENTIFIER
Chemicals, Peptides, and Recombinant Proteins		
G418	Amresco	Cat#97063-058
Nourseothricin	Amresco	Cat#6021-878
Hygromycin B	Amresco	Cat# 97064-454
Urea	Sigma-Aldrich	Cat#51456
RNase A	Sigma-Aldrich	Cat#R4875
Glass beads, acid-washed	Sigma-Aldrich	Cat#G8772
L-Arginine	Amresco	Cat#10118-198
L-Lysine	Amresco	Cat#97061-666
¹⁵ N ₄ ¹³ C ₆ -arginine	Cambridge Isotope Laboratories	Cat#DNLM-6801-PK
¹⁵ N ₂ ¹³ C ₆ -lysine	Cambridge Isotope Laboratories	Cat#CDNLM-6810-PK
SYTOX Green Dead Cell Stain	Invitrogen	Cat#S34860
Yeast Extract	Thermo Scientific	Cat#LP0021
Bacto peptone	BD	Cat#211677
Yeast Arg Lys minus	FunGenome Company	Cat#YGM003A-70
Critical Commercial Assays		
T5 Direct PCR Kit	Tsingke	Cat#TSE011
GeneArt seamless cloning and assembly enzyme mix	Invitrogen	Cat#A14606
TruSeq Nano DNA Library Prep Kit	Illumina	Cat#C-121-4001
TruSeq DNA Sample Prep Kit	Illumina	Cat#C-121-2003
TruSeq Stranded mRNA Library Prep Kit	Illumina	Cat#S-122-2101
Deposited Data		
RNA-seq raw data	this paper	GSA: CRA000490
DNA-seq raw data	this paper	GSA: CRA000490
Mass spectrometry proteomics data	this paper	ProteomeXchange: PXD007157
Experimental Models: Organisms/Strains		
<i>S. cerevisiae</i> : Strain background: Y12	Maclean et al. (2017)	PMID: 28472365
<i>S. cerevisiae</i> : Strain background: M22	Maclean et al. (2017)	PMID: 28472365
<i>S. cerevisiae</i> : Strain background: NCYC110	Maclean et al. (2017)	PMID: 28472365
<i>S. cerevisiae</i> : Strain background: UWOPS05-217.3	Maclean et al. (2017)	PMID: 28472365
<i>S. cerevisiae</i> : Strain background: BY4741	Brachmann et al. (1998)	PMID:9483801
<i>S. cerevisiae</i> : Strain background: BY4742	Brachmann et al. (1998)	PMID:9483801
<i>S. cerevisiae</i> : Strain background: BY4743	Brachmann et al. (1998)	PMID:9483801
Oligonucleotides		
Primers, see Table S7	this paper	N/A
Recombinant DNA		
pFA6a-GFP(S65T)-kanMX6	Bahler et al. (1998)	RRID: Addgene_39292
pAG25	Goldstein and McCusker (1999)	RRID: Addgene_35121
pAG32	Goldstein and McCusker (1999)	RRID: Addgene_35122
Software and Algorithms		
Matlab	MathWorks	https://www.mathworks.com/products/matlab.html
BWA	Li and Durbin (2009)	http://bio-bwa.sourceforge.net/

(Continued on next page)

Continued

REAGENT or RESOURCE	SOURCE	IDENTIFIER
GATK	McKenna et al. (2010)	https://software.broadinstitute.org/gatk/
Bowtie2	Langmead and Salzberg (2012)	http://bowtie-bio.sourceforge.net/bowtie2/index.shtml
Samtools	Li et al. (2009)	http://samtools.sourceforge.net/
MaxQuant	Cox et al. (2009)	https://www.biochem.mpg.de/5111795/maxquant
R	R Development Core Team	https://www.r-project.org/

LEAD CONTACT AND MATERIALS AVAILABILITY

Further information and requests for resources and reagents should be directed to and will be fulfilled by the Lead Contact, Lucas B. Carey (lucas.carey@pku.edu.cn).

Materials Availability Statement

This study did not generate new unique reagents.

METHOD DETAILS**Construction of Heterozygous $2n+x$ Strains**

To obtain $2n+x$ yeast strains, we first constructed a heterozygous $5n$ -Chr III strain. Three haploid strains (Y12 background, *MATa ho Δ 0::HygMX4*; M22 background, *MAT α ho Δ 0::KanMX4*; NCYC110 background, *MAT α ho Δ 0::HygMX4*) and a $2n$ -Chr III strain (UWOPS05-217.3 background, *MATa ho Δ 0::HygMX4*) were used. The $2n$ -Chr III strain contains 1 copy of chromosome III and 2 copies of the other 15 chromosomes. Because the locus determining the mating type of yeast (*MAT*) is on chromosome III, this $2n$ -Chr III strain can mate with a *MAT α* strain. The $5n$ -Chr III strain was constructed by two rounds of mating (Figure S1A). In the first round, a $2n$ strain was generated by crossing Y12 and NCYC110 and a $3n$ -Chr III strain was generated by crossing UWOPS05-217.3 and M22. After that, *MAT α* and *MATa* loci were knocked out in the $3n$ -Chr III and $2n$ strains, respectively. In the second round of mating, the $5n$ -Chr III strain was obtained by crossing the $2n$ and $3n$ -Chr III strains generated above. Three $5n$ -Chr III strains were independently generated. Interestingly, one of them gained a copy of Chr III and Chr VII and another lost a copy of Chr XIV. These initial strains were referred to as $5n$ for short hereafter and in the main text.

Heterozygous $5n$ cells were sporulated to generate $2n+x$ yeast strains. Cells were pre-grown in liquid YPD culture (1% yeast extract, 2% peptone, and 2% dextrose) and were transferred to the pre-sporulation media (1% yeast extract, 2% peptone, and 1% potassium acetate), where cells grew for 18-24h to reach the late log phase (1×10^7 to 2×10^7 cells/ml). Cells were harvested by centrifugation (3000g, 5 min) at room temperature and were washed twice with sterile distilled H_2O . Cells were further resuspended in the sporulation media (1% potassium acetate) at a final density of 1×10^7 to 2×10^7 cells/ml and were incubated in a shaking incubator at 30°C and 200 rpm for 4 days, after which tetrad dissections were performed.

Construction of Homozygous $2n+x$ Strains

To obtain homozygous $2n+x$ yeast strains, we first constructed a homozygous $5n$ strain. A $2n$ strains (BY4743 background, *his3 Δ 1 leu2 Δ 0 lys2 Δ 0 ura3 Δ 0*) and a $1n$ strain (BY4742 background, *MAT α ho Δ 0::URA3*) were used. Similar to the heterozygous $5n$ strain, the homozygous $5n$ strain was constructed by two rounds of mating (Figure S4A). In the first round, a $4n$ strain was generated by crossing two $2n$ strains in which *MAT α* and *MATa* loci were knocked out by KanMX and NatMX, respectively. The *MAT α* locus was further knocked out in the $4n$ strain by HygMX, and in the second round of mating, the $5n$ strain was obtained by crossing the $1n$ and $4n$ strains generated above. $5n$ cells were sporulated to generate homozygous $2n+x$ strains, after which tetrad dissections were performed. In parallel, $4n$ cells were also sporulated to generate $2n$ strains. The $2n$ strains were put on the same tetrad dissection plates with $2n+x$ strains to normalize the proliferation rate of aneuploidies on different plates.

Construction of Variants in a $2n+x$ Background

We performed a manipulative experiment that genetically changed a 3-copy protein complex to 2-copy or imbalanced in a $2n+x$ aneuploid strain. Strain 8-C was chosen because it is the only $2n+x$ aneuploidy among 40 heterozygous strains in this study that contains only one dominant selective marker (HygMX), and therefore, two genes can be deleted using KanMX and NatMX. Three 2-subunit protein complexes in which both subunits are present in three copies in strain 8-C were randomly chosen. For each complex, imbalanced variant (GFP-positive) was generated by deleting one copy of a subunit with KanMX & GFP. 2-copy (GFP-positive) variant was generated by deleting one copy of both subunits with KanMX & GFP and NatMX, respectively. A 3-copy variant was generated, in

which two copies of *HO* were knocked out with these two markers, respectively, in order to control for the effect of selective markers on proliferation rate. *HO* is a gene required for homothallic switching and is believed to have no effect on vegetative growth (Qian et al., 2012).

Construction of Variants in a 2n Background

Four 2-subunit protein complexes identified as overdosage sensitive complexes (Table S3) were randomly chosen. For each protein complex, one copy of a subunit (subunit1) was inserted at *HO* in BY4741 using KanMX as the selective marker, and one copy of the other (subunit2) was inserted at *HO* in BY4742 using NatMX as the marker. In parallel, strains with only KanMX and NatMX inserted at *HO* in BY4741 and BY4742 were also generated, respectively. 2-copy variant was generated by crossing BY4741 with KanMX and BY4742 with NatMX. Imbalanced variant was generated by crossing BY4741 with KanMX and BY4742 with subunit2 & NatMX or by crossing BY4741 with subunit1 & KanMX and BY4742 with NatMX. 3-copy variant was generated by crossing BY4741 with subunit1 & KanMX and BY4742 subunit2 & NatMX. All primers used in PCR-based gene replacement experiments in above sections were listed in Table S7.

DNA Sequencing

For DNA sequencing, 5 μ g of genomic DNA from each aneuploidy strain was prepared. Libraries of heterozygous $2n+x$ strains were generated with TruSeq Stranded mRNA Kit (Illumina) according to the manufacturer's instructions and were sequenced for paired-end sequencing on an Illumina HiSeq 2000 at BerryGenomics, Beijing, China. Libraries of homozygous $2n+x$ strains were generated with TruSeq Nano DNA Library Prep Kit (Illumina) and were sequenced with the NovaSeq 6000 sequencing system at BerryGenomics.

mRNA Sequencing

mRNA-seq was performed to quantify the mRNA abundance of 9 aneuploid strains. For RNA sequencing, 5 μ g of total RNA was used for poly(A)⁺ RNA selection. Stranded cDNA libraries were generated with TruSeq Stranded mRNA Kit (Illumina) according to the manufacturer's instructions. The cDNA libraries were sequenced for paired-end sequencing on an Illumina HiSeq 2000 at BerryGenomics.

SILAC

A strain for heavy isotope labeling (Lys8 and Arg10) was constructed on the background of BY4742 (*MAT α his3 Δ 1 leu2 Δ 0 lys2 Δ 0 ura3 Δ 0*), for SILAC analysis. BY4742 cannot synthesize lysine because *LYS2* was knocked out. We further knocked out *ARG4* and *CAR1* (*arg4 Δ 0::kanMX4 car1 Δ 0::LEU2*) so that this strain can neither synthesize arginine nor convert arginine to proline. Primers used in PCR-based gene replacement experiments were listed in Table S7.

Aneuploid cells were cultured overnight at 30°C in a synthetic complete medium in the presence of light amino acid isotopes (Lys0 and Arg0, 100 mg/ml each). The reference strain (BY4742 *MAT α his3 Δ 1 leu2 Δ 0 lys2 Δ 0 ura3 Δ 0 arg4 Δ 0::kanMX4 car1 Δ 0::LEU2*) was cultured similarly but in the presence of heavy amino acid isotopes (¹⁵N₂¹³C₆-lysine and ¹⁵N₄¹³C₆-arginine, Lys8 and Arg10 respectively for short). Cells were harvested at the mid-log phase (OD₆₆₀ = 0.6-0.8) and were resuspended in 150 μ l lysis buffer (8 M urea, 1 mM sodium orthovanadate, 1 mM sodium fluoride, 2.5 sodium pyrophosphate, 1 mM B-glycerophosphate, 0.2% tablet of protease inhibitor, and 1 mM PMSF). Subsequently, we mixed the cell lysate of each light amino acid-labeled $2n+x$ or $2n$ strain with that of the heavy amino acid-labeled reference strain under the 1:1 ratio. The mixed lysate was then sonicated for 20 min (with a basic cycle of 10 seconds on and 10 seconds off, 30% power) with an ultrasonic homogenizer (Scientz Biotechnology). After a centrifugation at 12,000 rpm for 20 min at 16°C, the supernatant was subject to the tandem mass spectrometry (MS/MS) analysis at the Proteome Core Facility at IGDB.

DNA Content Analysis Using Flow Cytometry

Aneuploid cells were cultured in YPD liquid media and 5×10^6 cells were harvested at the log phase. A $2n$ strain generated by crossing Y12 and NCYC110 and a $3n$ strain generated by crossing the $2n$ strain and M22 were harvested in parallel as the diploid and triploid reference genome. Cells were fixed with 200 μ l 70% ethanol for 1 h at room temperature, and were subsequently incubated in 200 μ l 50 μ g/ml RNase A solution for 3 h at 37°C and 200 μ l 50 μ g/ml proteinase K solution for 3 hours at 55°C. Both reagents were dissolved in 0.05 M sodium citrate. Samples were sonicated using an ultrasonic homogenizer (60% power) for 2 cycles (10 seconds on and 10 seconds off) to disperse cells evenly. Cells were stained with Sytox Green (Invitrogen) for 20 minutes following the manufacturer's instructions. Finally, DNA content was analyzed with flow cytometry (BD FACSAria II, excitation at 488 nm). The proportion of time in each cell-cycle stage was qualified by fitting the cell-cycle model with FlowJo.

QUANTIFICATION AND STATISTICAL ANALYSIS

Quantifying Proliferation Rate

Proliferation rates of 40 heterozygous $2n+x$ strains were estimated by calculating the areas of colonies, after a 4-day growth on the tetrad dissection plates. The images of 40 colonies were converted to binary images with the function "im2bw" in MATLAB (level = 0.7). The area of each colony was qualified with the function "regionprops". To control for batch effects across plates, the

proliferation rate of each strain was divided by the average proliferation rate of all $2n+x$ strains on the corresponding plate. Cells that separated in meiosis II usually had similar but not identical karyotypes and proliferation rates (Figures 1B, 1D, and 1E), probably due to sister chromatid mis-segregation or chromosome translocations during meiosis (Loidl, 1995). Therefore, they were treated as independent samples. The correlations between proliferation rate and other factors in this study were calculated for both Pearson's (r) and Kendall's Tau-a (τ). Proliferation rates of 52 homozygous $2n+x$ strains were estimated similarly, and their proliferation rates were further normalized by that of diploid strains.

Karyotyping Heterozygous $2n+x$ Aneuploidies

Paired-end reads (150 bp \times 2) were aligned to the SGD R64-2-1 S288C reference genome (Cherry et al., 2012) with the Burrows-Wheeler Aligner (BWA v0.7.12). The SNP information in the heterozygous strains was used to determine the copy number of each chromosome. To this end, the genomes of four parental strains (Y12, M22, NCYC110 and UWOPS05-217.3) were also sequenced. After sequencing reads were aligned to the S288C reference genome, the SNP information of these strains was obtained by SNP calling with GATK and SAMtools (Li, 2011; McKenna et al., 2010). Only concordant SNPs that were called by both tools were used for further analysis. In total, we identified 24751, 38179, 29333, and 33497 strain-specific SNPs that were unique in Y12, M22, NCYC110, and UWOPS05-217.3, respectively. We then divided each chromosome in a $2n+x$ strain into non-overlapping 1000 bp windows, and counted the number of strains that contributed to the DNA in each window based on their unique SNPs. If a chromosome contains more than 20 windows where SNPs are contributed by 3 strains, the chromosome was classified as a 3-copy chromosome. The classification was further manually curated. 3-copy chromosomes exhibited on average a ~ 1.5 fold sequencing read density of that of 2-copy chromosomes, suggesting that the genome remained stable at least in the first few rounds of cell division after sporulation. Some chromosomes are 1-copy and some are chimeric, with part of them 2-copy and the rest 3-copy, probably due to the mis-segregation or chromosome translocation during meiosis. For such chromosomes, the copy numbers of the regions with a larger size are shown in Figure 1D. It is worth noting that SNPs may potentially affect the proliferation rates of these $2n+x$ strains. Nevertheless, partial correlations between the number of additional genes and proliferation rate remained significant after controlling for the proportion of SNPs (Y22; M22; NCYC110; UWOPS05-217.3) from each parental strain in a $2n+x$ strain ($r = -0.45$, $P = 0.005$; $r = -0.51$ $P = 0.001$; $r = -0.51$ $P = 0.001$; $r = -0.50$ $P = 0.001$, respectively). Here, the SNP proportion of a parental strain in a $2n+x$ strain was calculated as the total number of reads matching the unique SNPs of the parental strain divided by the total number of reads covering the unique SNPs of this parental strain.

Karyotyping Homozygous $2n+x$ Aneuploidies

Genomic DNA of homozygous aneuploid strains was sequenced with the NovaSeq 6000 sequencing system. Paired-end reads (150 bp \times 2) were aligned to the SGD R64-2-1 S288C reference genome with the BWA (v0.7.16a-r1181). The average sequencing depths of non-overlapping 1,000 bp windows were calculated. The copy number of each chromosome was manually curated based on the fact that 3-copy chromosomes should exhibit a ~ 1.5 fold sequencing depths of that of 2-copy chromosomes on average.

Calculating Subcolonial Karyotype Variation

The fraction of cells with karyotype variation was estimated from the DNA-seq data. Specifically, the median sequencing depths of non-overlapping 1,000 bp windows on chromosome i was calculated. The sequencing coverage of one copy of each chromosome (H) were determined:

$$H = \frac{1}{2} \left(\frac{\sum_{i=1}^n A_i}{2n} + \frac{\sum_{i=1}^{16-n} B_i}{3(16-n)} \right),$$

where A_i was the median coverage of 2-copy chromosome i , and B_i was that of 3-copy chromosome i .

For each chromosome, the percentage of cells (P) in which this chromosome is 2-copy was calculated from the relationship:

$$A_i = 2HP + 3H(1 - P).$$

The fraction of cells (F) with chromosome i gains or losses was estimated:

$$F_i = \min(|P|, |1 - P|).$$

The max (F_i) was defined as the maximum possible fraction of cells with chromosome gains or losses.

Quantifying mRNA Abundance

Paired-end reads (150 bp \times 2) were aligned to the SGD R64-2-1 S288C reference genome (www.yeastgenome.org) using Tophat (v.2.1.0), allowing up to 5 mismatches. Transcript abundance, in the unit of Reads Per Kilobase per Million mapped reads (RPKM), was calculated with cufflinks (v2.2.1).

Quantifying Protein Abundance

MS/MS spectra were matched to the database containing the translated sequences of all predicted open reading frames in the *S. cerevisiae* genome (Cherry et al., 2012) and protein abundances were estimated with MaxQuant (v1.4.1.2) (Cox et al., 2009; de

Godoy et al., 2008). Search parameters allowed less than 2 missed cleavages and up to 3 labeled amino acids to be detected in a peptide sequence.

Estimating Relative Time in Cell-Cycle Stages

The proportion of time in each cell-cycle stage was qualified by fitting a cell-cycle model using FlowJo.

Data Retrieval

An up-to-date set of protein complexes in yeast (CYC2008 complexes set) was downloaded from <http://wodaklab.org/cyc2008/downloads> (Pu et al., 2009). Subunits encoded by genes on the mitochondrial genome were not included in this study. Genes from the WGD were retrieved from a previous study (Kellis et al., 2004). The karyotypes and proliferation rates of $n+x$ aneuploid strains (in rich media at 23°C) were retrieved from the study by Pavelka et al. and were downloaded from the Open Data Repository (ODR) of the Stowers Institute for Medical Research (<http://odr.stowers.org/websimr/>). The data of copy number variation in cancer cells were downloaded from The Cancer Genome Atlas (TCGA) database (Cancer Genome Atlas Research Network et al., 2013), which includes the information of 22,457 human cancer samples across 26 cancer types. The information of 1,521 protein complexes in humans was downloaded from HPRD release 9 (www.hprd.org). 1,317 of them were annotated completely and were used in this study. Chromosomal locations of these genes were retrieved from Ensembl release 87 (www.ensembl.org).

DATA AND CODE AVAILABILITY

The accession number for the high-throughput sequencing data reported in this paper is GSA: CRA000490 (<http://bigd.big.ac.cn/gsa>) (Wang et al., 2017). The accession number for the mass spectrometry proteomics data reported in this paper is ProteomeXchange: PXD007157 (<http://proteomecentral.proteomexchange.org>) (Vizcaino et al., 2013).